

Seasonal Dynamics of Epiphytic Microbial Communities on Marine Macrophyte Surfaces

^{1†}

† To whom correspondence should be addressed: marino.korlevic@irb.hr

1. Ruđer Bošković Institute, Center for Marine Research, G. Paliaga 5, Rovinj, Croatia
2. University of Vienna, Department of Limnology and Bio-Oceanography, Althanstraße 14, Vienna, Austria

1 **Abstract**

2 Introduction

3 Marine macrophytes (seagrasses and macroalgae) are important ecosystem engineers that
4 form close associations with microorganism belonging to all three domains of life (Egan *et al.*,
5 2013; Tarquinio *et al.*, 2019). Microbes can live within macrophyte tissue as endophytes or can
6 form epiphytic communities on surfaces of leaves and thalli (Egan *et al.*, 2013; Hollants *et al.*,
7 2013; Tarquinio *et al.*, 2019). Epiphytic and endophytic microbial communities form a close
8 functional relationship with the macrophyte host. It was proposed that this close relationship
9 constitutes a holobiont, an integrated community where the macrophyte organism and its symbiotic
10 partners support each other (Margulis, 1991; Egan *et al.*, 2013; Tarquinio *et al.*, 2019).

11 Biofilms formed from microbial epiphytes can contain diverse taxonomic groups and harbor
12 cell densities from 10^2 to 10^7 cells cm^{-2} (Armstrong *et al.*, 2000; Bengtsson *et al.*, 2010; Burke *et*
13 *al.*, 2011b). In such an environment a number of positive and negative interactions between the
14 macrophyte and colonizing microorganisms have been described (Egan *et al.*, 2013; Hollants *et*
15 *al.*, 2013; Tarquinio *et al.*, 2019). Macrophytes can promote growth of associated microbes by
16 nutrient exudation, while in return microorganisms may support macrophyte performance through
17 improved nutrient availability, phytohormone production and protection form toxic compounds,
18 oxidative stress, biofouling organisms and pathogens (Egan *et al.*, 2013; Hollants *et al.*, 2013;
19 Tarquinio *et al.*, 2019). Beside this positive interactions, macrophytes can negatively impact
20 the associated microbes such as pathogenic bacteria by producing reactive oxygen species and
21 secondary metabolites (Egan *et al.*, 2013; Hollants *et al.*, 2013; Tarquinio *et al.*, 2019).

22 All these ecological roles are carried out by a taxonomically diverse community of
23 microorganisms. At higher taxonomic ranks a core set of macrophyte epiphytic taxa was
24 described consisting mainly of *Alphaproteobacteria*, *Gammaproteobacteria*, *Desulfobacterota*,
25 *Bacteroidota*, *Cyanobacteria*, *Actinobacteriota*, *Firmicutes*, *Planctomyctota*, *Chloroflexi* and
26 *Verrucomicrobiota* (Crump and Koch, 2008; Tujula *et al.*, 2010; Lachnit *et al.*, 2011). In contrast,

27 at lower taxonomic ranks host specific microbial communities were described (Lachnit *et al.*,
28 2011; Roth-Schulze *et al.*, 2016). Recently, it was shown that even different morphological niches
29 within the same alga had a higher influence on bacterial community variation than biogeography
30 or environmental factors (Morrissey *et al.*, 2019). While there is high community variation
31 between host species is was observed that the majority of metagenomes determined functions
32 were conserved both between host species and individuals (Burke *et al.*, 2011a; Roth-Schulze *et*
33 *al.*, 2016). This discrepancy between taxonomic and functional composition could be explained
34 by the lottery hypothesis. It postulates that an initial random colonization step is performed from
35 a set of functionally equivalent taxonomic groups resulting in taxonomically different epiphytic
36 communities sharing a core set of functional genes (Burke *et al.*, 2011a; Roth-Schulze *et al.*,
37 2016). In addition, some of the variation in the observed data could be attributed to different
38 techniques used in various studies, such as different protocols for epiphytic cell detachment and/or
39 DNA isolation, as no standard protocol to study epiphytic communities was established (Ugarelli
40 *et al.*, 2019; Korlević *et al.*, submitted).

41 The majority of studies describing macrophyte epiphytic communities did not encompass
42 seasonal changes (Crump and Koch, 2008; Lachnit *et al.*, 2009; Burke *et al.*, 2011b; Roth-Schulze
43 *et al.*, 2016; Ugarelli *et al.*, 2019). In addition, if seasonal changes were taken into account
44 low temporal frequency and/or methodologies that do not allow for high taxonomic resolution
45 were used (Tujula *et al.*, 2010; Lachnit *et al.*, 2011; Miranda *et al.*, 2013). In the present study
46 we describe the seasonal dynamics of bacterial and archaeal communities on the surfaces of
47 the seagrass *Cymodocea nodosa* and siphonous macroalgae *Caulerpa cylindracea* determined
48 on a mostly monthly scale. Bacterial and archaeal epiphytes were sampled in a meadow of
49 *Cymodocea nodosa* invaded by the invasive *Caulerpa cylindracea* and in a locality of only
50 *Caulerpa cylindracea* located in the proximity of the meadow. In addition, for comparison the
51 community of the surrounding seawater was characterized.

52 **Materials and Methods**

53 **Sampling**

54 Leaves of *Cymodocea nodosa* were sampled in a *Cymodocea nodosa* meadow located in the
55 proximity of the village of Funtana (45°10'39" N, 13°35'42" E). Thalli of *Caulerpa cylindracea*
56 were sampled in the same *Cymodocea nodosa* invaded meadow in Funtana and on a locality of
57 only *Caulerpa cylindracea* located close to the invaded meadow. Sampling of leaves and thalli
58 was performed approximately monthly from December 2017 to October 2018. Leaves and thalli
59 were collected by diving and transported to the laboratory in containers placed on ice and filled
60 with site seawater. Upon arrival to the laboratory, *Cymodocea nodosa* leaves were cut into sections
61 of 1 – 2 cm, while *Caulerpa cylindracea* thalli were cut into 5 – 8 cm long sections. Leaves and
62 thalli were washed three times with sterile artificial seawater (ASW) to remove loosely attached
63 microbial cells. Surrounding seawater was collected in 10 l containers by diving and transported to
64 the laboratory where the whole container volume was filtered through a 20 µm net. The filtrate was
65 further sequentially filtered through 3 µm and 0.2 µm polycarbonate membrane filters (Whatman,
66 United Kingdom) using a peristaltic pump. Filters were briefly dried at room temperature and
67 stored at –80 °C. Seawater samples were also collected approximately monthly from July 2017 to
68 October 2018.

69 **DNA Isolation**

70 DNA from surfaces of *Cymodocea nodosa* and *Caulerpa cylindracea* was isolated using a
71 previously modified and adapted protocol that allows a selective epiphytic DNA isolation (Massana
72 *et al.*, 1997; Korlević *et al.*, submitted). Briefly, leaves and thalli are incubated in a lysis buffer
73 and treated with lysozyme and proteinase K. Following the incubations, the mixture containing
74 lysed epiphytic cells is separated from leaves and thalli and extracted using a phenol-chloroform

75 procedure. Finally, the extracted DNA is precipitated using isopropanol. DNA from seawater
76 picoplankton was isolated from 0.2 μ m polycarbonate filters according to (Massana *et al.*, 1997)
77 with a slight modification. Following the phenol-chloroform extraction steps 1/10 of chilled 3
78 M sodium acetate (pH 5.2) was added. DNA was precipitated by adding 1 volume of chilled
79 isopropanol, incubating the mixtures overnight at -20 °C and centrifuging at 20,000 \times g and 4 °C
80 for 21 min. The pellet was washed twice with 500 μ l of chilled 70 % ethanol and centrifuged after
81 each washing step at 20,000 \times g and 4 °C for 5 min. Dried pellets were resuspended in 50 – 100 μ l
82 of deionized water.

83 **Illumina 16S rRNA Sequencing**

84 Illumina MiSeq sequencing of the V4 16S rRNA region was performed as described
85 previously (Korlević *et al.*, submitted). The V4 region of the 16S rRNA gene was amplified using
86 a two-step PCR procedure. In the first PCR the 515F (5'-GTGYCAGCMGCCGCGTAA-3')
87 and 806R (5'-GGACTACNVGGGTWTCTAAT-3') primers from the Earth Microbiome Project
88 (<http://press.igsb.anl.gov/earthmicrobiome/protocols-and-standards/16s/>) were used to amplify
89 the target region (Caporaso *et al.*, 2012; Apprill *et al.*, 2015; Parada *et al.*, 2016). These primers
90 contained on their 5' end a tagged sequence. Purified PCR products were sent for Illumina MiSeq
91 sequencing at IMGM Laboratories, Martinsried, Germany. Before sequencing, the second PCR
92 amplification of the two-step PCR procedure was performed at IMGM using primers targeting
93 the tagged region incorporated in the first PCR. In addition, these primers contained adapter
94 and sample-specific index sequences. Beside samples, a positive and negative control for each
95 sequencing batch were sequenced. A negative control was comprised of PCR reactions without
96 DNA template, while for a positive controls a mock community composed of evenly mixed DNA
97 material originating from 20 bacterial strains (ATCC MSA-1002, ATCC, USA) was used. The
98 sequences obtained in this study have been submitted to the European Nucleotide Archive (ENA)
99 under accession numbers **TO BE ADDED LATER!**.

100 **Sequence Analysis**

101 Obtained sequences were analyzed on the computer cluster Isabella (University Computing
102 Center, University of Zagreb) using mothur (version 1.43.0) (Schloss *et al.*, 2009) according
103 to the MiSeq Standard Operating Procedure (MiSeq SOP; https://mothur.org/wiki/MiSeq_SOP)
104 (Kozich *et al.*, 2013) and recommendations given from the Riffomonas project to enhance data
105 reproducibility (<http://www.riffomonas.org/>). For alignment and classification of sequences the
106 SILVA SSU Ref NR 99 database (release 138; <http://www.arb-silva.de>) was used (Quast *et al.*,
107 2013; Yilmaz *et al.*, 2014). Pipeline data processing and visualization was done using R (version
108 3.6.0) (R Core Team, 2019), package vegan (version 2.5-6) (Oksanen *et al.*, 2019), package
109 tidyverse (version 1.3.0) (Wickham *et al.*, 2019) and multiple other packages (Xie, 2014, 2015,
110 2019a, 2019b, 2020; Neuwirth, 2014; Xie *et al.*, 2018; Allaire *et al.*, 2019; Zhu, 2019). The
111 detailed analysis procedure including the R Markdown file for this paper are available as a GitHub
112 repository (**TO BE ADDED LATER!**). Based on the ATCC MSA-1002 mock community
113 included in the analysis an average sequencing error rate of 0.01 % was determined, which is in
114 line with previously reported values for next-generation sequencing data (Kozich *et al.*, 2013;
115 Schloss *et al.*, 2016). In addition, the negative controls processed together with the samples
116 yielded on average only 2 sequences after sequence quality curation.

117 **Results**

118 Sequencing of the 16S rRNA V4 region yielded a total of 1.8 million sequences after
119 sequence quality curation and exclusion of eukaryotic, chloroplast, mitochondrial and no relative
120 sequences. A total of 35 samples originating from epiphytic archaeal and bacterial communities
121 associated with surfaces of the seagrass *Cymodocea nodosa* and macroalga *Caulerpa cylindracea*
122 were analyzed. In addition, 18 samples (one of the samples was sequenced two times) originating
123 from picoplankton archaeal and bacterial communities in the surrounding seawater were also

124 processed. The number of reads per sample ranged between 8,407 and 77,465 sequences. Even
125 when the highest sequencing effort was applied the rarefaction curves did not level off that is a
126 common observation in high-throughput 16S rRNA amplicon sequencing approaches (Figure S1).
127 Following quality curation and exclusion of sequences mentioned before reads were clustered
128 into 28,726 different OTUs at a similarity level of 97 %. Reads numbers were normalized to the
129 minimum number of sequences, 8,407, through rarefaction resulting in 17,158 different OTUs
130 that ranged from 373 to 2,088 OTUs per sample (Figure S2). To determine seasonal changes of
131 richness and diversity in studied environments the Observed Number of OTUs, Chao1, ACE,
132 Exponential Shannon (Jost, 2006) and Inverse Simpson were calculated after normalization
133 through rarefaction.

134 To determine the proportion of shared archaeal and bacterial OTUs and shared archaeal
135 and bacterial communities sampled in different environments (*Cymodocea nodosa* [Invaded],
136 *Caulerpa cylindracea* [Invaded and Noninvaded] and surrounding seawater) the Jaccard's
137 Similarity Coefficient on presence-absence data and Bray-Curtis Similarity Coefficient were,
138 respectively, calculated. Similarity coefficients were determined after normalization through
139 rarefaction and binning of samples from a respective environment. The highest proportion of
140 shared OTUs and communities was found between *Caulerpa cylindracea* invaded and noninvaded
141 meadow communities (Jaccard, 0.35; Bray-Curtis, 0.77), while lower shared values were
142 calculated between seawater and epiphytic communities (Figure 1). Shared proportions of OTUs
143 and communities between *Cymodocea nodosa* and *Caulerpa cylindracea* were approximately in
144 the middle between these two extremes.

145 To assess seasonal changes in the proportion of shared bacterial and archaeal OTUs the
146 Jaccard's Similarity Coefficient was calculated between consecutive sampling points (Figure 2).

¹⁴⁷ **Discussion**

¹⁴⁸ **Acknowledgments**

149 **References**

- 150 Allaire, J.J., Xie, Y., McPherson, J., Luraschi, J., Ushey, K., Atkins, A., et al. (2019)
- 151 rmarkdown: Dynamic Documents for R.
- 152 Apprill, A., McNally, S., Parsons, R., and Weber, L. (2015) Minor revision to V4 region
- 153 SSU rRNA 806R gene primer greatly increases detection of SAR11 bacterioplankton. *Aquatic*
- 154 *Microbial Ecology* **75**: 129–137.
- 155 Armstrong, E., Rogerson, A., and Leftley, J.W. (2000) The Abundance of Heterotrophic
- 156 Protists Associated with Intertidal Seaweeds. *Estuarine, Coastal and Shelf Science* **50**: 415–424.
- 157 Bengtsson, M., Sjøtun, K., and Øvreås, L. (2010) Seasonal dynamics of bacterial biofilms on
- 158 the kelp *Laminaria hyperborea*. *Aquatic Microbial Ecology* **60**: 71–83.
- 159 Burke, C., Steinberg, P., Rusch, D., Kjelleberg, S., and Thomas, T. (2011a) Bacterial
- 160 community assembly based on functional genes rather than species. *Proceedings of the National*
- 161 *Academy of Sciences of the United States of America* **108**: 14288–14293.
- 162 Burke, C., Thomas, T., Lewis, M., Steinberg, P., and Kjelleberg, S. (2011b) Composition,
- 163 uniqueness and variability of the epiphytic bacterial community of the green alga *Ulva australis*.
- 164 *The ISME journal* **5**: 590–600.
- 165 Caporaso, J.G., Lauber, C.L., Walters, W.A., Berg-Lyons, D., Huntley, J., Fierer, N., et al.
- 166 (2012) Ultra-high-throughput microbial community analysis on the Illumina HiSeq and MiSeq
- 167 platforms. *The ISME Journal* **6**: 1621–1624.
- 168 Crump, B.C. and Koch, E.W. (2008) Attached bacterial populations shared by four species of
- 169 aquatic angiosperms. *Applied and environmental microbiology* **74**: 5948–5957.
- 170 Egan, S., Harder, T., Burke, C., Steinberg, P., Kjelleberg, S., and Thomas, T. (2013) The

¹⁷¹ seaweed holobiont: understanding seaweed-bacteria interactions. *FEMS microbiology reviews* **37**:
¹⁷² 462–476.

¹⁷³ Hollants, J., Leliaert, F., De Clerck, O., and Willems, A. (2013) What we can learn from
¹⁷⁴ sushi: A review on seaweed-bacterial associations. **83**: 1–16.

¹⁷⁵ Jost, L. (2006) Entropy and diversity. **113**: 363–375.

¹⁷⁶ Korlević, M., Markovski, M., Zhao, Z., Herndl, G.J., and Najdek, M. Selective DNA and
¹⁷⁷ Protein Isolation from Marine Macrophyte Surfaces.

¹⁷⁸ Kozich, J.J., Westcott, S.L., Baxter, N.T., Highlander, S.K., and Schloss, P.D. (2013)
¹⁷⁹ Development of a dual-index sequencing strategy and curation pipeline for analyzing amplicon
¹⁸⁰ sequence data on the MiSeq Illumina sequencing platform. *Applied and environmental*
¹⁸¹ *microbiology* **79**: 5112–5120.

¹⁸² Lachnit, T., Blümel, M., Imhoff, J.F., and Wahl, M. (2009) Specific epibacterial communities
¹⁸³ on macroalgae: Phylogeny matters more than habitat. *Aquatic Biology* **5**: 181–186.

¹⁸⁴ Lachnit, T., Meske, D., Wahl, M., Harder, T., and Schmitz, R. (2011) Epibacterial community
¹⁸⁵ patterns on marine macroalgae are host-specific but temporally variable. *Environmental*
¹⁸⁶ *Microbiology* **13**: 655–665.

¹⁸⁷ Margulis, L. (1991) Symbiogenesis and symbiontism. In, Margulis,L. and Fester,R. (eds),
¹⁸⁸ *Symbiosis as a source of evolutionary innovation*. Cambridge, Massachusetts: The MIT Press, pp.
¹⁸⁹ 1–14.

¹⁹⁰ Massana, R., Murray, A.E., Preston, C.M., and DeLong, E.F. (1997) Vertical distribution and
¹⁹¹ phylogenetic characterization of marine planktonic Archaea in the Santa Barbara Channel. *Applied*
¹⁹² *and environmental microbiology* **63**: 50–56.

¹⁹³ Miranda, L.N., Hutchison, K., Grossman, A.R., and Brawley, S.H. (2013) Diversity and

194 Abundance of the Bacterial Community of the Red Macroalga *Porphyra umbilicalis*: Did Bacterial
195 Farmers Produce Macroalgae? *PLoS ONE* **8**: e58269.

196 Morrissey, K.L., Çavas, L., Willems, A., and De Clerck, O. (2019) Disentangling the influence
197 of environment, host specificity and thallus differentiation on bacterial communities in siphonous
198 green seaweeds. *Frontiers in Microbiology* **10**:

199 Neuwirth, E. (2014) RColorBrewer: ColorBrewer Palettes.

200 Oksanen, J., Blanchet, F.G., Friendly, M., Kindt, R., Legendre, P., McGlinn, D., et al. (2019)
201 vegan: Community Ecology Package.

202 Parada, A.E., Needham, D.M., and Fuhrman, J.A. (2016) Every base matters: assessing small
203 subunit rRNA primers for marine microbiomes with mock communities, time series and global
204 field samples. *Environmental Microbiology* **18**: 1403–1414.

205 Quast, C., Pruesse, E., Yilmaz, P., Gerken, J., Schweer, T., Yarza, P., et al. (2013) The SILVA
206 ribosomal RNA gene database project: improved data processing and web-based tools. *Nucleic
207 acids research* **41**: D590–6.

208 R Core Team (2019) R: A Language and Environment for Statistical Computing, Vienna,
209 Austria: R Foundation for Statistical Computing.

210 Roth-Schulze, A.J., Zozaya-Valdés, E., Steinberg, P.D., and Thomas, T. (2016) Partitioning of
211 functional and taxonomic diversity in surface-associated microbial communities. *Environmental
212 microbiology* **18**: 4391–4402.

213 Schloss, P.D., Girard, R.A., Martin, T., Edwards, J., and Thrash, J.C. (2016) Status of the
214 Archaeal and Bacterial Census: an Update. *mBio* **7**: e00201–16.

215 Schloss, P.D., Westcott, S.L., Ryabin, T., Hall, J.R., Hartmann, M., Hollister, E.B., et al.
216 (2009) Introducing mothur: open-source, platform-independent, community-supported software

217 for describing and comparing microbial communities. *Applied and environmental microbiology*
218 **75**: 7537–7541.

219 Tarquinio, F., Hyndes, G.A., Laverock, B., Koenders, A., and Säwström, C. (2019) The
220 seagrass holobiont: Understanding seagrass-bacteria interactions and their role in seagrass
221 ecosystem functioning. *FEMS Microbiology Letters* **366**:

222 Tujula, N.A., Crocetti, G.R., Burke, C., Thomas, T., Holmström, C., and Kjelleberg, S. (2010)
223 Variability and abundance of the epiphytic bacterial community associated with a green marine
224 Ulvacean alga. *The ISME Journal* **4**: 301–311.

225 Ugarelli, K., Laas, P., and Stingl, U. (2019) The microbial communities of leaves and roots
226 associated with turtle grass (*Thalassia testudinum*) and manatee grass (*syringodium filliforme*) are
227 distinct from seawater and sediment communities, but are similar between species and sampling
228 sites. *Microorganisms* **7**:

229 Wickham, H., Averick, M., Bryan, J., Chang, W., McGowan, L.D., François, R., et al. (2019)
230 Welcome to the tidyverse. *Journal of Open Source Software* **4**: 1686.

231 Xie, Y. (2015) Dynamic Documents with {R} and knitr, 2nd ed. Boca Raton, Florida:
232 Chapman; Hall/CRC.

233 Xie, Y. (2014) knitr: A Comprehensive Tool for Reproducible Research in {R}. In,
234 Stodden, V., Leisch, F., and Peng, R.D. (eds), *Implementing reproducible computational research*.
235 Chapman; Hall/CRC.

236 Xie, Y. (2019a) knitr: A General-Purpose Package for Dynamic Report Generation in R.

237 Xie, Y. (2019b) TinyTeX: A lightweight, cross-platform, and easy-to-maintain LaTeX
238 distribution based on TeX Live. *TUGboat* 30–32.

239 Xie, Y. (2020) tinytex: Helper Functions to Install and Maintain 'TeX Live', and Compile

²⁴⁰ 'LaTeX' Documents.

²⁴¹ Xie, Y., Allaire, J.J., and Grolemund, G. (2018) R Markdown: The Definitive Guide, Boca
²⁴² Raton, Florida: Chapman; Hall/CRC.

²⁴³ Yilmaz, P., Parfrey, L.W., Yarza, P., Gerken, J., Pruesse, E., Quast, C., et al. (2014) The SILVA
²⁴⁴ and "All-species Living Tree Project (LTP)" taxonomic frameworks. *Nucleic acids research* **42**:
²⁴⁵ D643–8.

²⁴⁶ Zhu, H. (2019) kableExtra: Construct Complex Table with 'kable' and Pipe Syntax.

247 **Figure Captions**

248 **Figure 1.** Proportion of shared bacterial and archaeal OTUs (Jaccard's Similarity Coefficient)
249 and shared bacterial and archaeal communities (Bray-Curtis Similarity Coefficient) between
250 communities associated with the surfaces of macrophytes (*Cymodocea nodosa* [Invaded] and
251 *Caulerpa cylindracea* [Invaded and Noninvaded]) and coomunities in the surrounding seawater.

252 **Figure 2.** Proportion of shared bacterial and archaeal communities (Bray-Curtis Similarity
253 Coefficient) and shared bacterial and archaeal OTUs (Jaccard's Similarity Coefficient) between
254 consecutive sampling points and from the surfaces of macrophytes (*Cymodocea nodosa* [Invaded]
255 and *Caulerpa cylindracea* [Invaded and Noninvaded]) and in the surrounding seawater.

256 **Figure 3.** Principal Coordinates Analysis (PCoA) of Bray-Curtis distances based on OTU
257 abundances of bacterial and archaeal communities from the surfaces of macrophytes (*Cymodocea*
258 *nodosa* [Invaded] and *Caulerpa cylindracea* [Invaded and Noninvaded]) and in the surrounding
259 seawater. Samples from the same environment or same season are labeld in different colors. The
260 proportion of explained variation by each axis is shown on the corresponding axis in parentheses.

261 **Figure 4.** Taxonomic classification and relative contribution of the most abundant bacterial and
262 archaeal sequences on the surfaces of macrophytes (*Cymodocea nodosa* [Invaded] and *Caulerpa*
263 *cylindracea* [Invaded and Noninvaded]) and in the surrounding seawater.

264 **Figure 5.** Taxonomic classification and relative contribution of the most abundant cyanobacterial
265 sequences on the surfaces of macrophytes (*Cymodocea nodosa* [Invaded] and *Caulerpa*
266 *cylindracea* [Invaded and Noninvaded]) and in the surrounding seawater. The proportion of
267 cyanobacterial sequences in the total bacterial and archaeal community is given above the
268 corresponding bar. NR – No Relative

269 **Figure 6.** Taxonomic classification and relative contribution of the most abundant sequences
270 within the *Bacteroidota* on the surfaces of macrophytes (*Cymodocea nodosa* [Invaded] and

271 *Caulerpa cylindracea* [Invaded and Noninvaded]) and in the surrounding seawater. The proportion
272 of sequences classified as *Bacteroidota* in the total bacterial and archaeal community is given
273 above the corresponding bar. NR – No Relative

274 **Figure 7.** Taxonomic classification and relative contribution of the most abundant alphaproteobacterial
275 sequences on the surfaces of macrophytes (*Cymodocea nodosa* [Invaded] and *Caulerpa*
276 *cylindracea* [Invaded and Noninvaded]) and in the surrounding seawater. The proportion of
277 alphaproteobacterial sequences in the total bacterial and archaeal community is given above the
278 corresponding bar. NR – No Relative

279 **Figure 8.** Taxonomic classification and relative contribution of the most abundant gammaproteobacterial
280 sequences on the surfaces of macrophytes (*Cymodocea nodosa* [Invaded] and *Caulerpa*
281 *cylindracea* [Invaded and Noninvaded]) and in the surrounding seawater. The proportion of
282 gammaproteobacterial sequences in the total bacterial and archaeal community is given above the
283 corresponding bar. NR – No Relative

284 **Figure 9.** Taxonomic classification and relative contribution of the most abundant sequences
285 within the *Desulfobacterota* on the surfaces of macrophytes (*Cymodocea nodosa* [Invaded] and
286 *Caulerpa cylindracea* [Invaded and Noninvaded]) and in the surrounding seawater. The proportion
287 of sequences classified as *Desulfobacterota* in the total bacterial and archaeal community is given
288 above the corresponding bar. NR – No Relative

289 **Figures**

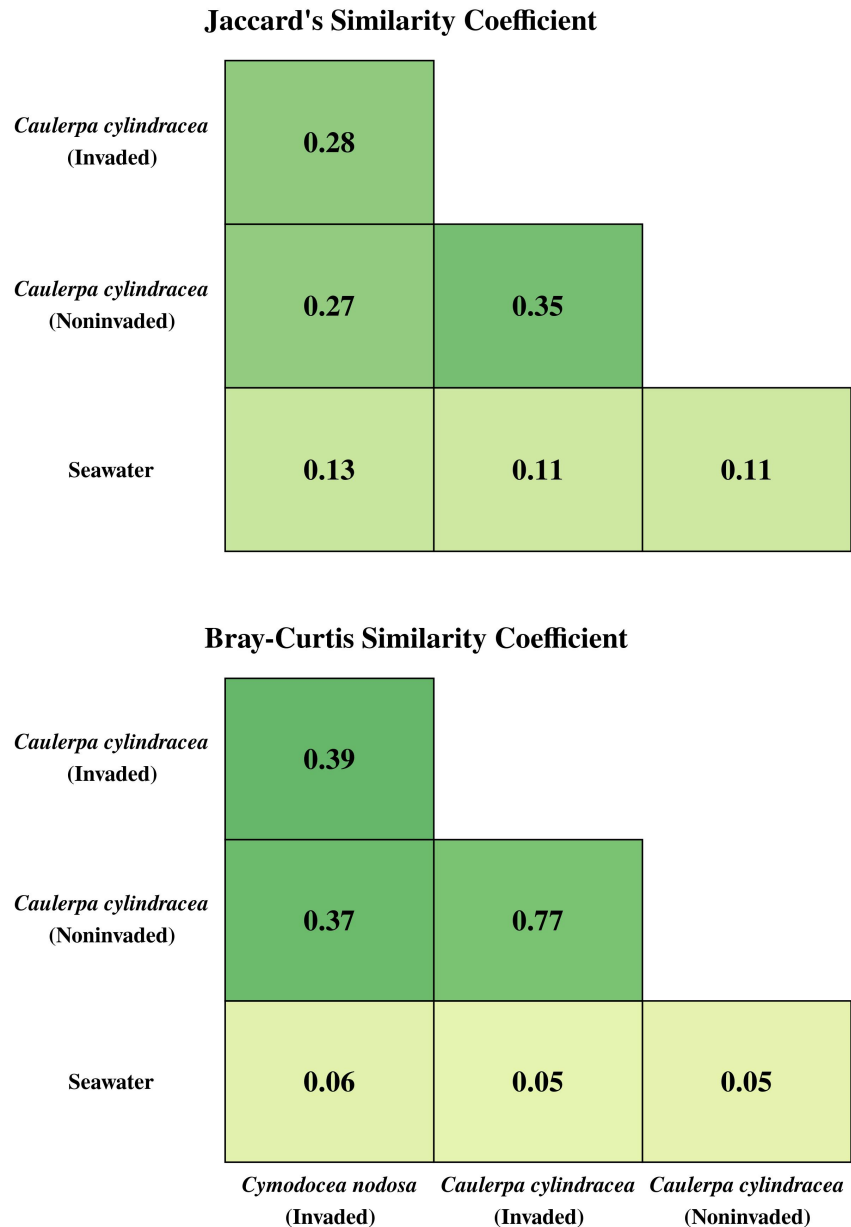


Figure 1. Proportion of shared bacterial and archaeal OTUs (Jaccard's Similarity Coefficient) and shared bacterial and archaeal communities (Bray-Curtis Similarity Coefficient) between communities associated with the surfaces of macrophytes (*Cymodocea nodosa* [Invaded] and *Caulerpa cylindracea* [Invaded and Noninvaded]) and coomunities in the surrounding seawater.

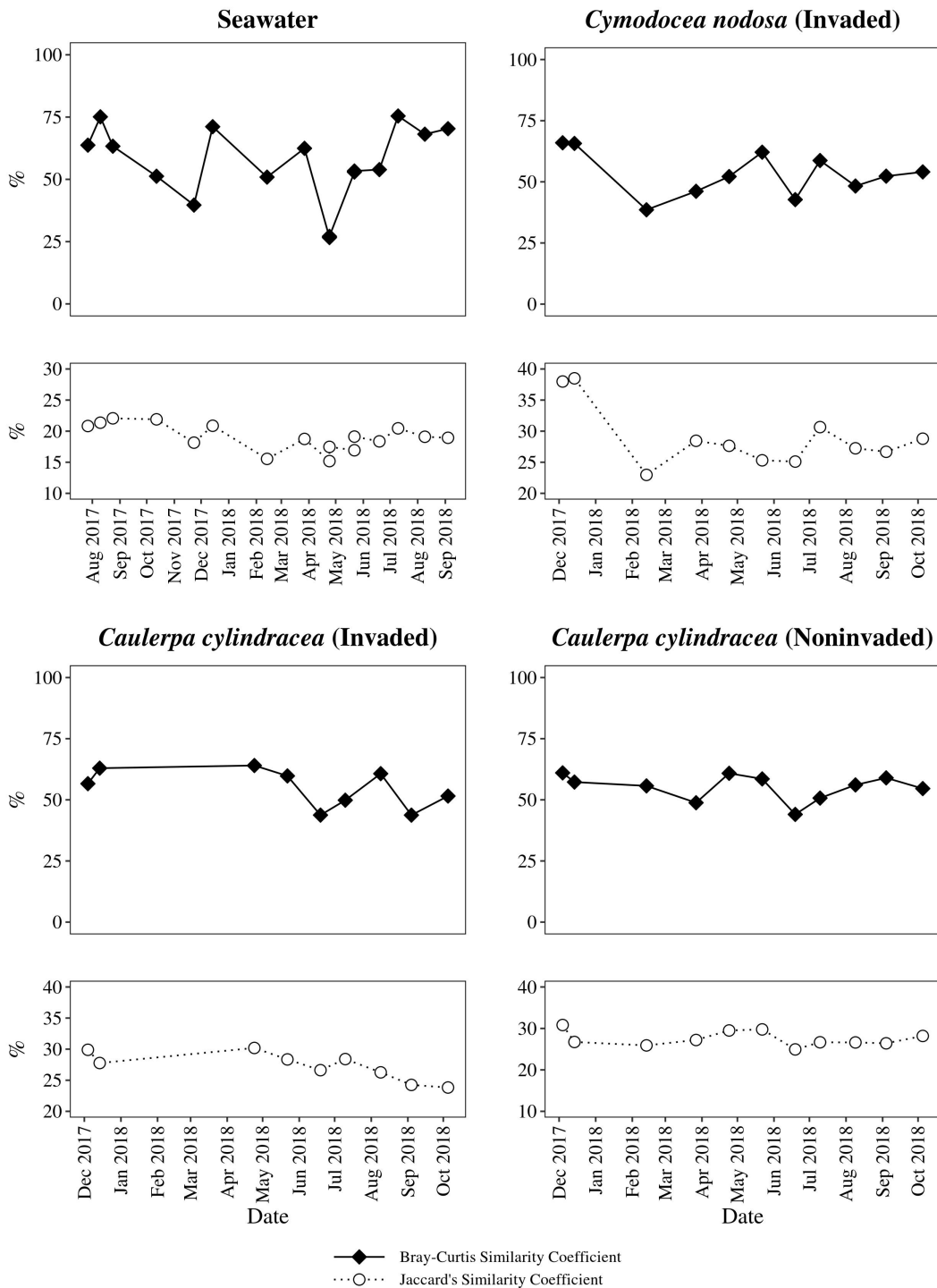


Figure 2. Proportion of shared bacterial and archaeal communities (Bray-Curtis Similarity Coefficient) and shared bacterial and archaeal OTUs (Jaccard's Similarity Coefficient) between consecutive sampling points and from the surfaces of macrophytes (*Cymodocea nodosa* [Invaded] and *Caulerpa cylindracea* [Invaded and Noninvaded]) and in the surrounding seawater.

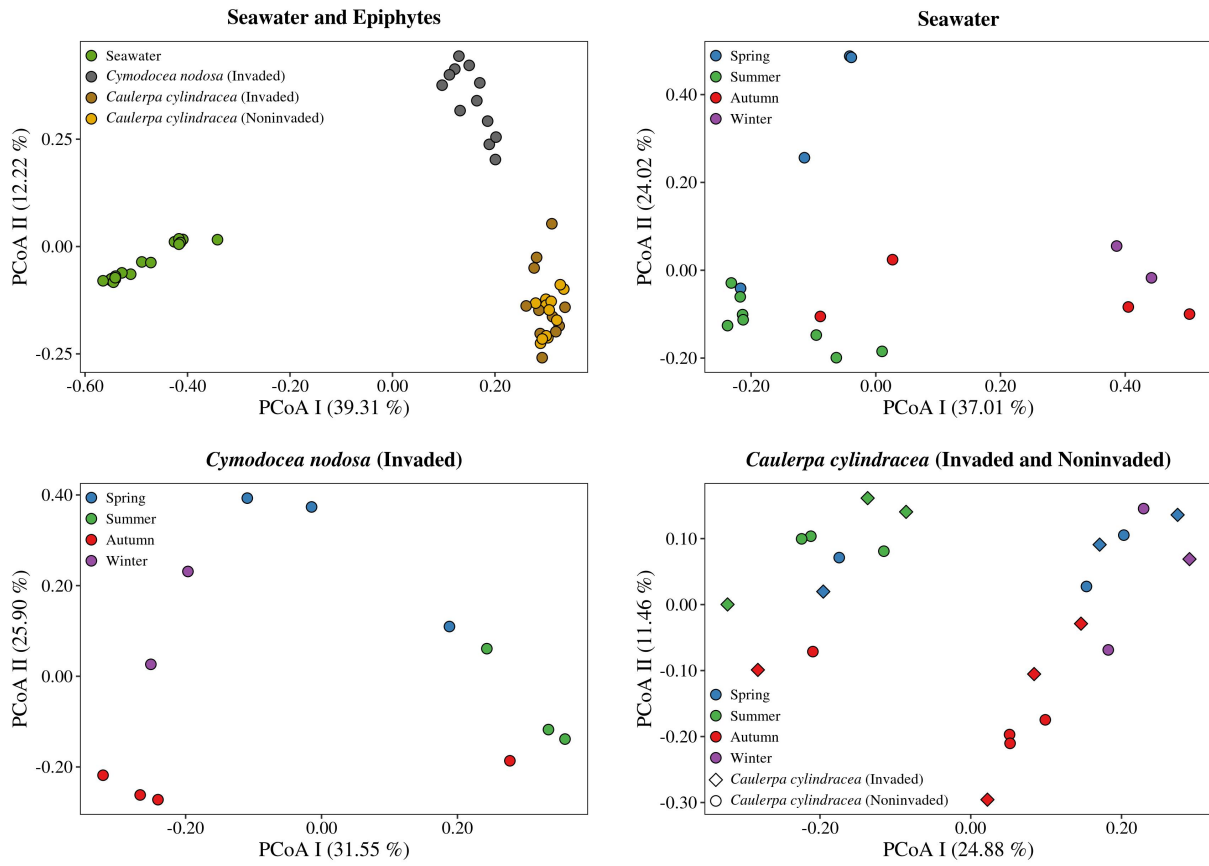


Figure 3. Principal Coordinates Analysis (PCoA) of Bray-Curtis distances based on OTU abundances of bacterial and archaeal communities from the surfaces of macrophytes (*Cymodocea nodosa* [Invaded] and *Caulerpa cylindracea* [Invaded and Noninvaded]) and in the surrounding seawater. Samples from the same environment or same season are labeled in different colors. The proportion of explained variation by each axis is shown on the corresponding axis in parentheses.

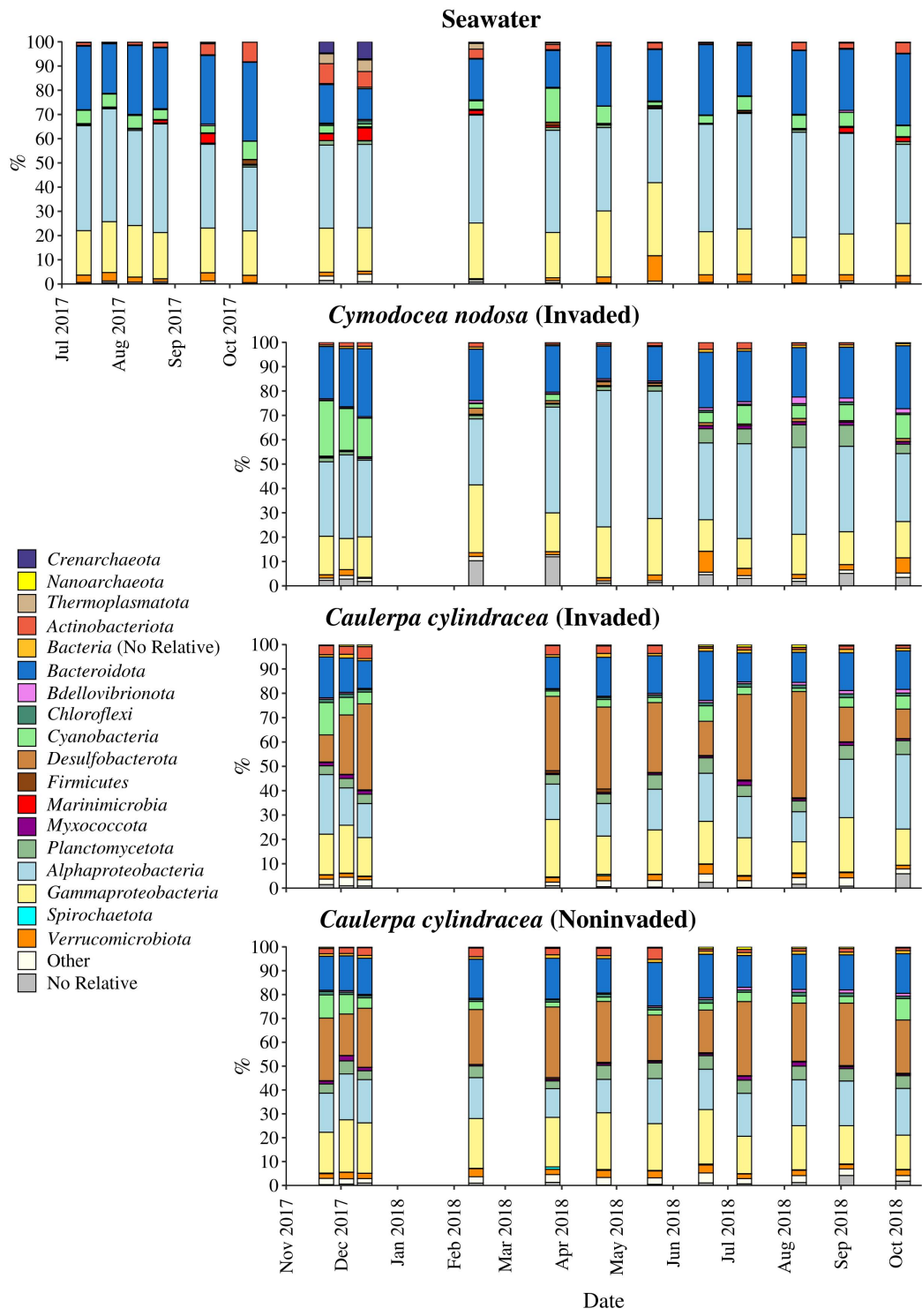


Figure 4. Taxonomic classification and relative contribution of the most abundant bacterial and archaeal sequences on the surfaces of macrophytes (*Cymodocea nodosa* [Invaded] and *Caulerpa cylindracea* [Invaded and Noninvaded]) and in the surrounding seawater.

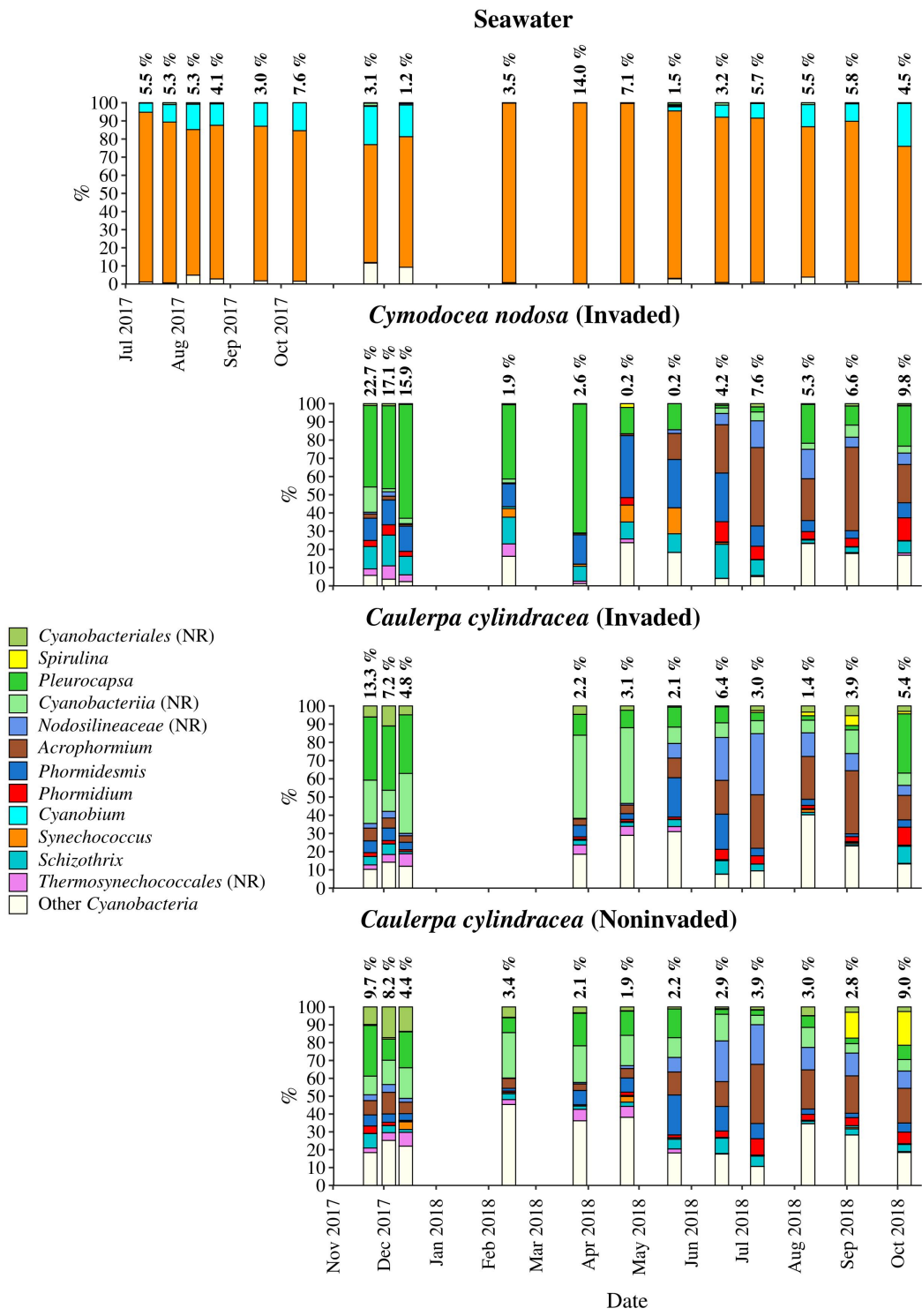


Figure 5. Taxonomic classification and relative contribution of the most abundant cyanobacterial sequences on the surfaces of macrophytes (*Cymodocea nodosa* [Invaded] and *Caulerpa cylindracea* [Invaded and Noninvaded]) and in the surrounding seawater. The proportion of cyanobacterial sequences in the total bacterial and archaeal community is given above the corresponding bar. NR – No Relative

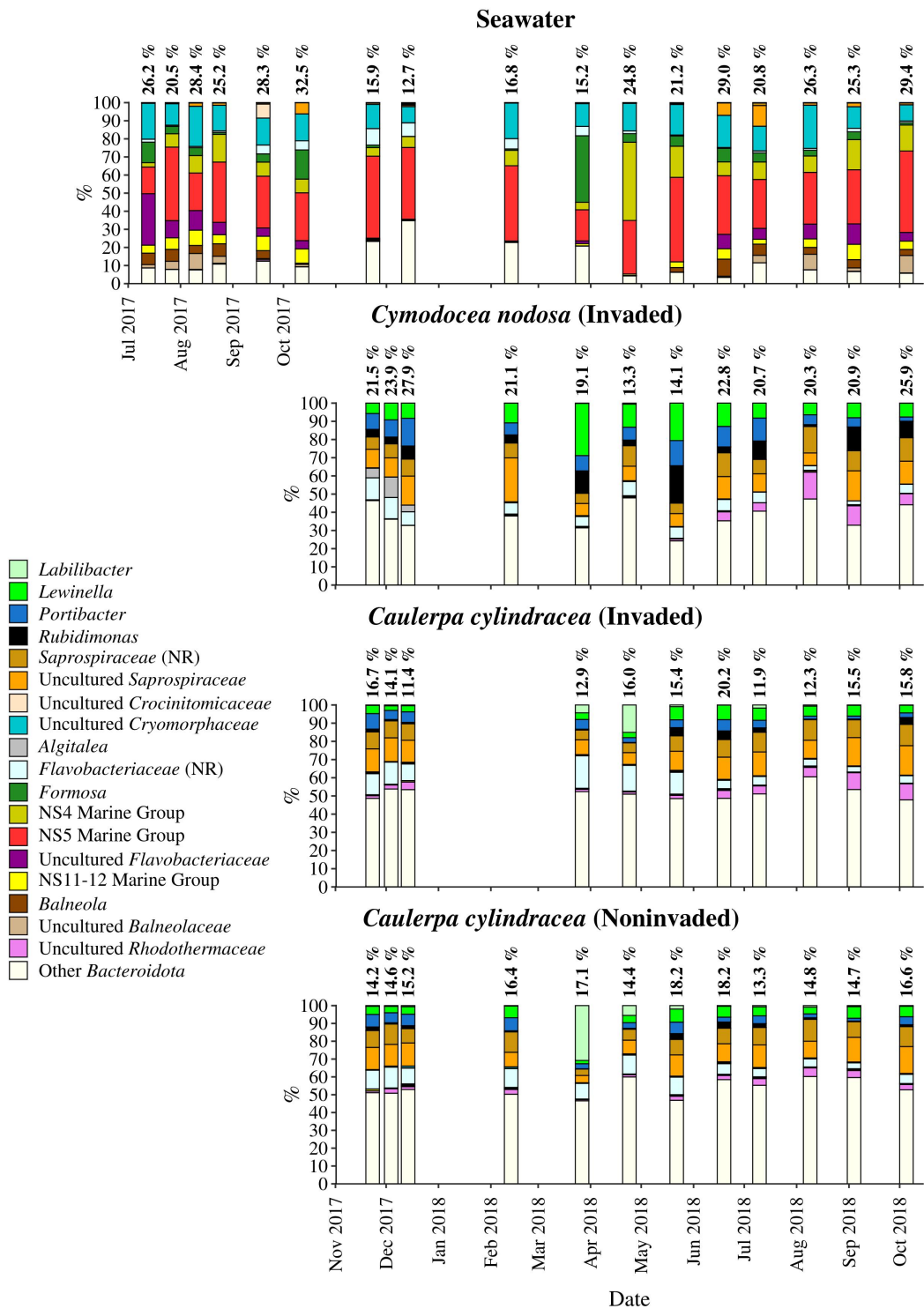


Figure 6. Taxonomic classification and relative contribution of the most abundant sequences within the *Bacteroidota* on the surfaces of macrophytes (*Cymodocea nodosa* [Invaded] and *Caulerpa cylindracea* [Invaded and Noninvaded]) and in the surrounding seawater. The proportion of sequences classified as *Bacteroidota* in the total bacterial and archaeal community is given above the corresponding bar. NR – No Relative

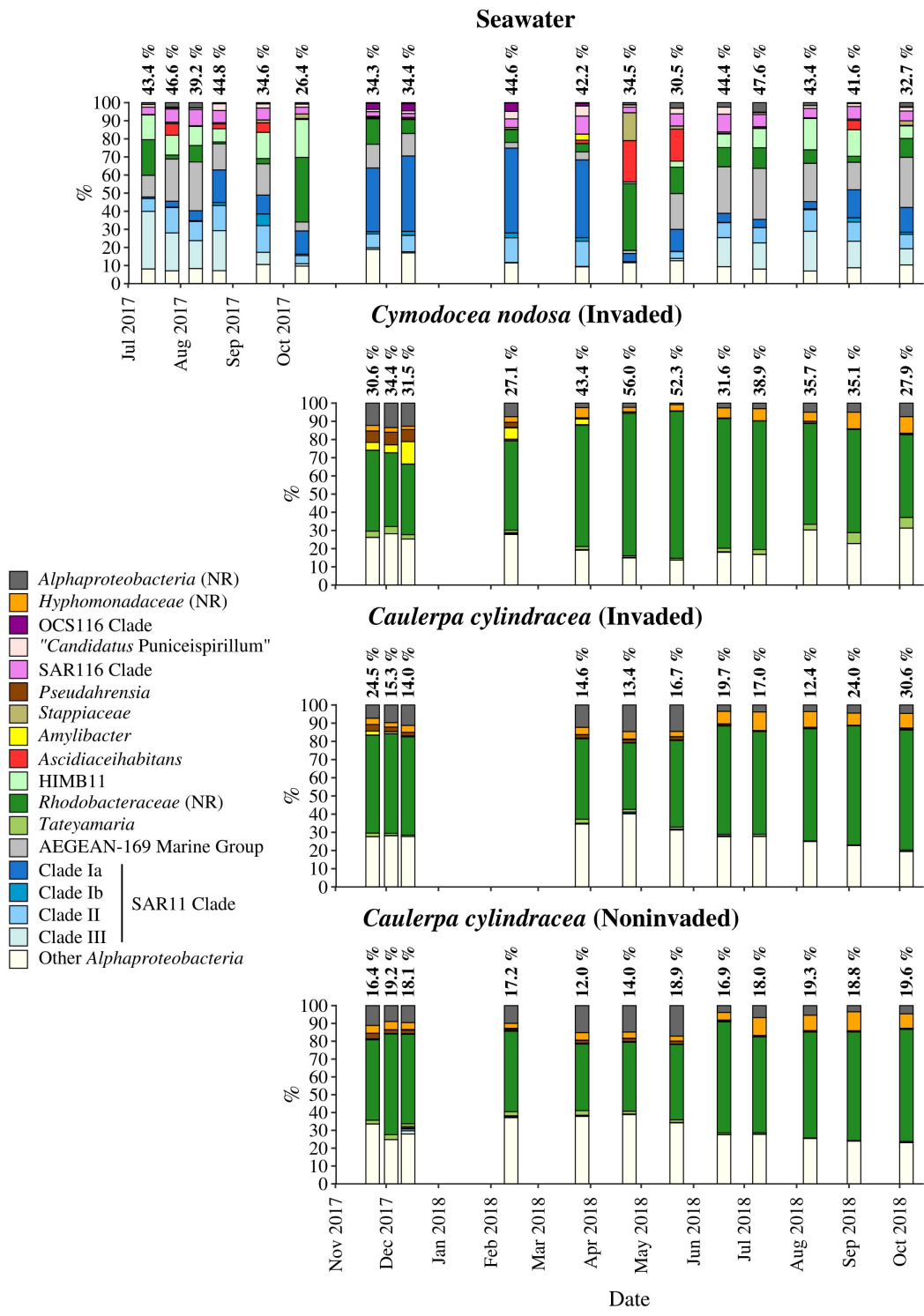


Figure 7. Taxonomic classification and relative contribution of the most abundant alphaproteobacterial sequences on the surfaces of macrophytes (*Cymodocea nodosa* [Invaded] and *Caulerpa cylindracea* [Invaded and Noninvaded]) and in the surrounding seawater. The proportion of alphaproteobacterial sequences in the total bacterial and archaeal community is given above the corresponding bar. NR – No Relative

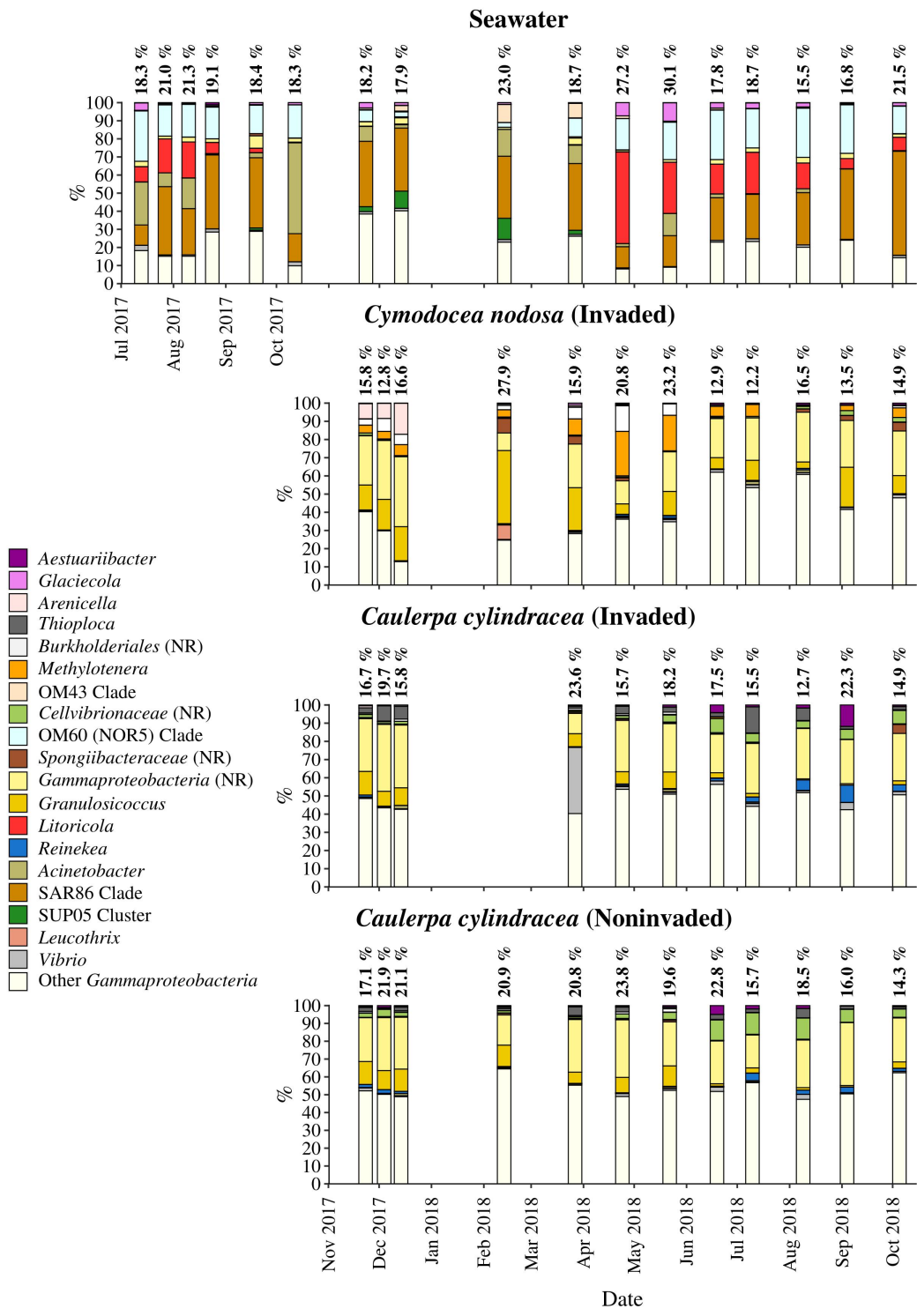


Figure 8. Taxonomic classification and relative contribution of the most abundant gammaproteobacterial sequences on the surfaces of macrophytes (*Cymodocea nodosa* [Invaded] and *Caulerpa cylindracea* [Invaded and Noninvaded]) and in the surrounding seawater. The proportion of gammaproteobacterial sequences in the total bacterial and archaeal community is given above the corresponding bar. NR – No Relative

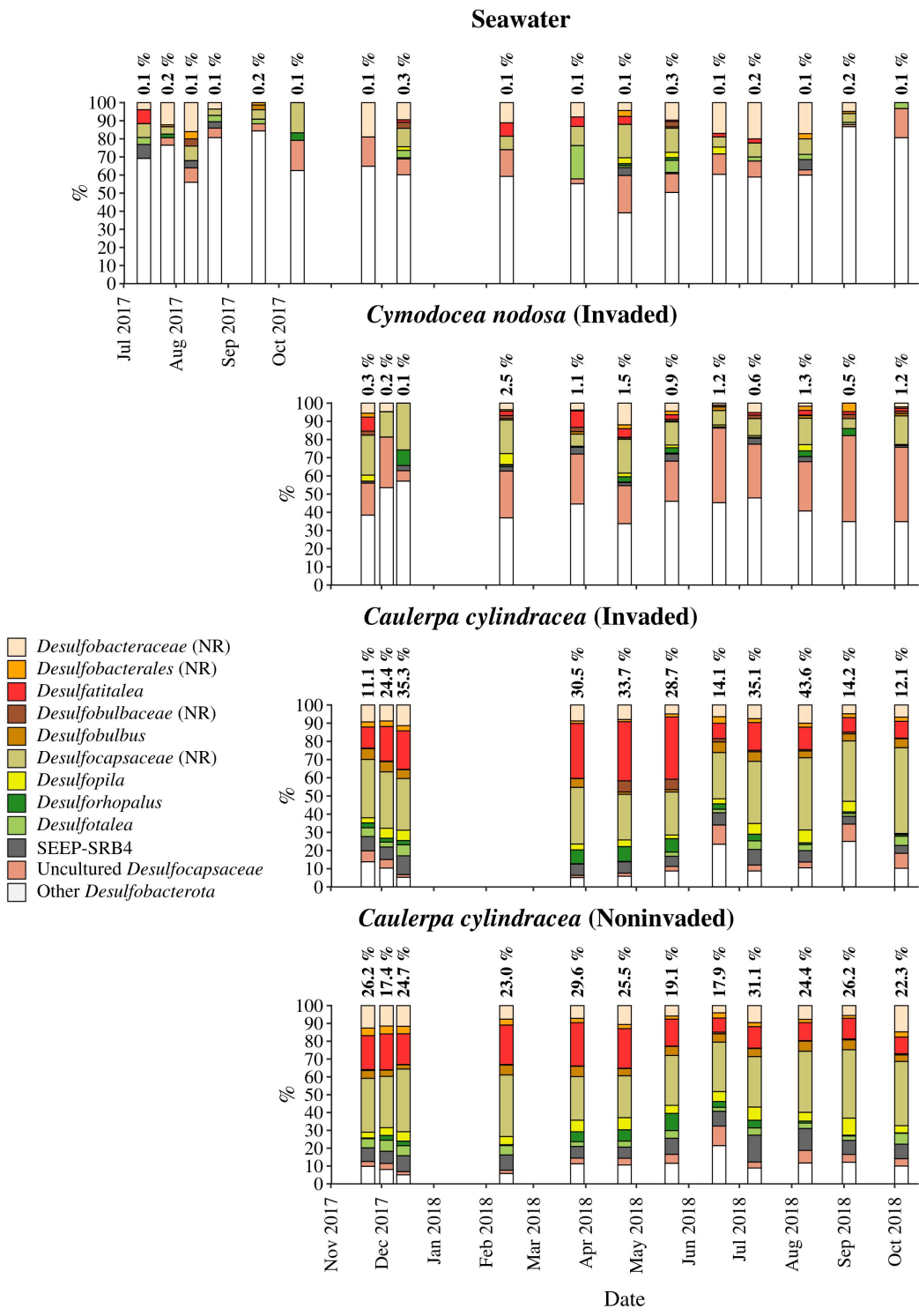


Figure 9. Taxonomic classification and relative contribution of the most abundant sequences within the *Desulfobacterota* on the surfaces of macrophytes (*Cymodocea nodosa* [Invaded] and *Caulerpa cylindracea* [Invaded and Noninvaded]) and in the surrounding seawater. The proportion of sequences classified as *Desulfobacterota* in the total bacterial and archaeal community is given above the corresponding bar. NR – No Relative